Mechanics of Advanced Composite Structures

An Analytical Study on the Indentation of a Layered Composite Beam and its Utilization in Low Velocity Impact Response

M. Hosseini*, A. Ahmadvand

Department of Mechanical Engineering, Faculty of Engineering, Malayer University, Malayer, Postcode65719-95863, Iran

K E Y W O R D S

A B S T R A C T

In the present paper, for the first time, the contact problem of a rigid cylindrical indenter and a laminated composite beam is solved using an assumed contact stress approach. Results are presented for contact force - contact length relation and contact stresses. Then, the results of the analysis are generalized to determine the low velocity impact response. The close agreement observed between the present results and those which existed in the literature, confirms the validity and the accuracy of the present analysis. Performing a parametric study, the effects of some important parameters on the indentation and the low velocity impact responses of the composite beam are investigated and discussed. The results reveal that the lay-up [90/90 90/90] gives the maximum contact length and the minimum contact pressure, but, conversely, the lay-up [0/0/0/0] produces the minimum contact length and the maximum contact pressure. The results of the present research can be of great importance in the design and application of layered composite beams.

1. Introduction

Composite structures are widely used in aircraft or vehicle bodies. During work or repair, rigid objects such as stones, tools, ... may strike these structures. The damages of these impacts in composite structures are more than those of metal structures. These impacts cause internal damages such as the delamination of the composite layers. Because the deformations are in the elastic (linear) range, the outer surface of the structure does not reveal these damages [1]. Hence, before composite structures can effectively be designed and used, it is essential that their behavior against static and dynamic loading be properly identified.

Apetre et al. [2] investigated the low velocity impact response of a sandwich beam with an FGM core. The projectile was a rigid cylinder and the impact was applied vertically. In their study, the core had variable Young modulus along with the thickness and the Poisson's ratio was constant. To solve the problem, static contact and impact response combination were employed as a simple dynamic solution based on quasi-static behavior, using a nonlinear mass and spring model, and the problem was solved by combining the Fourier series and Glerkin's principle. The results show that the contact stiffness of the beam with FGM core increases the contact stress in the vicinity of the contact zone. The value of the corresponding maximum strains for the maximum impact load is significantly reduced, due to the FG material. For a better comparison, the FGM core thickness was chosen so that the bending stiffness is equivalent to a beam with a homogeneous core and the results showed the better function of the FGM core, and the damages were significantly reduced.

Liu et al. [3] presented an impact theory model at the center of a sandwich beam for predicting the dynamic response. The core of the beam was thick and its strength was also low. In their research, two beams with medium and low strength cores were used and the beams were modeled based on two principles of Euler-Bernoulli and Galerkin and the responses of

---

impacts were compared. By the impact, the contact area of the projectile and the beam deformed plastically and the other side of the beam experienced elastic vibration. The results indicated that the dynamic response of the sandwich beam is highly sensitive to the core strength, the rate of the mass change, the geometric size variations, and the projectile velocity. The results of the theoretical analysis were in good agreement with the finite element simulations.

Ghazifard et al. [4] presented the results of a study by finite element analysis on energy absorption characteristics of hollow and foam-filled thin-walled structures subjected to quasi-static crushing load. It was observed that the energy absorption and initial peak force are influenced by foam density.

The classic theory of contact mechanics is the Hertzian mechanics' theory [5, 6]. In 1882, Hertz solved the problem of contacting two rigid bodies with curved surfaces. Hertz, based on the similarity of the linear elasticity equations with static electricity equations, guessed that the contact area should be elliptical. The response form can be found proportional to the dimensionless parameters, by dimensional analysis. This analysis shows that the contact area is related to the vertical force of the contact. But Hertz's theory provides a closed form precise analytical result. The classical contact theory ignores the friction and the cohesion effects of the contact surfaces. The theory of contact mechanics for composite structures is the expansion of the contact theories for the homogeneous structures, which these theories themselves have been derived from the expansion of Hertzian classical theory of contact mechanics.

Abrate [7, 8] in two comprehensive papers, had a complete review of impact dynamics and the response of composite structures to impact load, as well as how to study the start and growth of damage, the reduction of residual strength, and failure modes. As the deformation is important near the impact zone, the impact problem needs to be modeled and solved by an appropriate method in order to obtain strain, stress, displacement, and impact force versus time. This issue was first examined by Timoshenko. In this research, an isotropic beam with a determined length under impact loading was studied. He modeled the corresponding structure as a classic beam, ignoring the effects of shear deformation and rotary inertia. He also used Hertz law for the impact between the beam and the sphere and obtained deflection and curvature of the beam at the impact point in terms of an infinite series of vertical vibrational modes. The impact force was

calculated step by step with the solution of the integral equation [9].

In order to easily solve the impact problem, many researches consider the load to be concentrated. For example, in order to simplify the solution of the mathematical equations, Mittal [10], assumed that the dynamic load of the impact to be concentrated. In this case, it is clear that the curvatures and the strains tend to infinity and become very large. Therefore, it is necessary to consider the contact force to be distributed over the contact surface. If the impactor and the target are isotropic, the contact area will be circular.

Ivañez et al. [11] presented an analytical study of the low velocity impact response of a sandwich beam. In this study, dimensional analysis was performed to identify key parameters that affect the dynamic response of the beam. For determining the effects of dimensionless parameters on the contact force and the contact time factors, the predicted results were in good agreement with the experimental data for the maximum contact force, contact time, and contact force-time curve. It was observed that the parameters global stiffness, local stiffness, and impact velocity have the highest effect on the maximum force and the contact time.

Mines et al. [12] studied the sandwich composite beam behavior under impact loading and static loading, with different face sheets and with two types of cores. They examined the different modes of damages in each case and compared them.

Many previous, both empirical and analytical, studies have shown the relationship and similarity of static contact problems to the behavior of low velocity impact [13-17]. In this context, the main issue is that due to the negligible and non-deductible effects of wave propagation in low velocity impact, contact force – contact length and contact force – indentation depth relationships for static and dynamic problems are almost the same. Also, the stresses are similar in the vicinity of the contact area, which is why the same damage models are created in quasi-static and dynamic impact phenomena [15]. Therefore, the tolerance of damages due to impacts can be characterized by either static indentation tests or static contact analytical studies.

In the present paper firstly, the problem of contact between a rigid cylindrical indenter and a layered composite beam is analytically solved using an assumed contact stress approach. Then, the results of the analysis are extended to determine the low velocity impact response. Also, by conducting a parametric study, the effects of some key parameters on the indentation and the low velocity impact responses of the composite beam are studied.

2. Problem Statement

The problem of contacting a beam and an indenter is schematically shown in Fig. 1. The length of the beam is assumed L and its thickness h. Boundary conditions are considered as simple support. According to this figure, the considered composite beam is subjected to a smooth cylindrical indenter with the radius R at the center of its lower surface.

The goal is extracting the relationship between the contact force F and the contact length 2b, determining the stress field distributed in the beam for the known contact force, and also using the indentation analysis results to obtain the response of the low velocity impact problem.
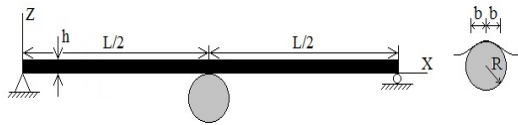
Fig. 1. Composite beam subjected to a rigid indenter

3. Problem Formulation

3.1. Indentation Analysis

The governing equations of motion are as the following two equations of equilibrium [18]:

$$\frac{\partial \sigma_{xx}}{\partial x} + \frac{\partial \tau_{xz}}{\partial z} = 0, \qquad \frac{\partial \sigma_{zz}}{\partial z} + \frac{\partial \tau_{xz}}{\partial x} = 0 \qquad (1)$$

Often the multi-layers are typically thin and follow the plane stress state. By ignoring σ_{22}, the governing elastic equation for the k-th layer of an orthotropic multi-layer is [19]:

$$\begin{Bmatrix} \sigma_1 \\ \sigma_3 \\ \sigma_5 \end{Bmatrix} = \begin{bmatrix} Q_{11} & Q_{13} & 0 \\ Q_{13} & Q_{33} & 0 \\ 0 & 0 & Q_{55} \end{bmatrix} \begin{Bmatrix} \varepsilon_1 \\ \varepsilon_3 \\ \varepsilon_5 \end{Bmatrix} \qquad (2)$$

where, $Q_{ij}^{(k)}$, is the lamina stiffness, σ_i, stress components, and ε_i the strain components. $Q_{ij}^{(k)}$ is related to the mechanical properties of materials using the following equations [19]:

$$Q_{11}^k = \frac{E_1^k}{1 - v_{11}^k v_{31}^k}, \qquad Q_{13}^k = \frac{v_{13}^k E_1^k}{1 - v_{13}^k v_{31}^k}$$

$$Q_{33}^k = \frac{E_3^k}{1 - v_{13}^k v_{31}^k}, \qquad Q_{55}^k = G_{13}^k \qquad (3)$$

The transformed stress-strain relations of an orthotropic lamina in the plane stress state are [19]:

$$\begin{Bmatrix} \sigma_{xx} \\ \sigma_{zz} \\ \sigma_{xz} \end{Bmatrix} = \begin{bmatrix} \bar{Q}_{11} & \bar{Q}_{13} & 0 \\ \bar{Q}_{13} & \bar{Q}_{33} & 0 \\ 0 & 0 & \bar{Q}_{55} \end{bmatrix} \begin{Bmatrix} \varepsilon_{xx} \\ \varepsilon_{yy} \\ \gamma_{xz} \end{Bmatrix} \qquad (4)$$

The strain-displacement equations are as follows [19]:

$$\varepsilon_{xx} = \frac{\partial u}{\partial x}, \quad \varepsilon_{zz} = \frac{\partial w}{\partial z}, \quad \gamma_{xz} = \frac{\partial u}{\partial z} + \frac{\partial w}{\partial x} \qquad (5)$$

By replacing equations (4) in (1) and using equations (5), the governing differential equations of the problem are obtained as follows:

$$\frac{\partial}{\partial x}\left(\bar{Q}_{11} \frac{\partial u}{\partial x} + \bar{Q}_{13} \frac{\partial w}{\partial z} \right) +$$

$$\frac{\partial}{\partial z}\left(\bar{Q}_{55} \frac{\partial u}{\partial z} + \bar{Q}_{55} \frac{\partial w}{\partial x} \right) = 0,$$

$$\frac{\partial}{\partial x}\left(\bar{Q}_{55} \frac{\partial u}{\partial z} + \bar{Q}_{55} \frac{\partial w}{\partial x} \right) + \qquad (6)$$

$$\frac{\partial}{\partial z}(\bar{Q}_{13} \frac{\partial u}{\partial x} + \bar{Q}_{33} \frac{\partial w}{\partial z}) = 0$$

According to Fig. 1, the boundary conditions at the ends of the beam (at $x = 0$ and $x = L$) are:

$$w(0, z) = w(L, z) = 0,$$

$$\sigma_{xx}(0, z) = \sigma_{xx}(L, z) = 0 \qquad (7)$$

The stress at the top surface of the beam is zero:

$$\sigma_{zz}(x, h) = \tau_{xz}(x, h) = 0 \qquad (8)$$

At the lower surface of the beam, where the impact also occurs, the boundary conditions are slightly more complicated. At the bottom surface, the shear stress τ_{xz} is zero and the normal stress σ_{zz} vanishes outside the contact zone, but in the contact zone, the displacement profile conforms to the shape of the rigid indenter. These boundary conditions can be written as:

$$\tau_{xz}(x, 0) = 0 \qquad (9)$$

$$\sigma_{zz}(x, 0) = 0, \qquad |\chi| > b \qquad (10)$$

$$\chi = x\text{-}L/2 \qquad (11)$$

$$w(x, 0) = \Delta - \frac{\chi^2}{2R}, \qquad |\chi| \le b \qquad (12)$$

where, $|\chi| > b$ is outside the contact region, $|\chi| \le b$ within the contact region, Δ the indenter displacement, and $2b$ the contact length.

It is worth mentioning that to simplify the investigation of the contact problem, the variable $\chi = x - \frac{L}{2}$ is introduced. Accordingly, the point $\chi = 0$ implies the center of the beam. As shown in Eq. (12), the indenter profile in the contact region is approximated as a parabola which is legal when the half contact length b is much smaller than the indenter radius R.

The contact problem is analyzed using the assumed contact stress approach. The contact stresses are assumed as [18]:

$$p_z(x) = -\sigma_{zz}(x,0) = \sum_{i=1}^{N} p_i \varphi_i(x), \quad |\chi| \le b \quad (13)$$

where φ_i's are known functions of x and p_i are constants that must be determined to satisfy the condition given in Eq. (12). Since $\Delta = w(\frac{L}{2}, 0)$, the contact conditions in the contact area can then be written as:

$$w\left(\frac{L}{2}, 0\right) - w(x, 0) = \frac{\chi^2}{2R}, \qquad |\chi| \le b \quad (14)$$

In order to determine the values of p_i it is assumed that the contact condition to be satisfied in M points $x = x_j$ on the contact surface.

$$w\left(\frac{L}{2}, 0\right) - w(x_j, 0) = \frac{\chi_j^2}{2R}, \qquad |\chi_j| \le b$$
$$(j = 1, M; \ M \ge N) \quad (15)$$

where $\chi_j = x_j - L/2$ the deflection of the beam at the contact surface can be written by the linear combination of the unknown compression coefficients P_i as:

$$\sum_{i=1}^{N} (c_{0i} - c_{ji}) p_i = \frac{\chi_j^2}{2R}, \qquad (j = 1, M; \ M \ge N) \quad (16)$$

where c_{0i} is the central displacement $w(\frac{L}{2}, 0)$ and c_{ji} is the displacement $w(x_j, 0)$ at x_j due to unit p_i. By solving the system of linear equations (16), one can obtain the values of p_i.

Here, the displacement fields $u(x,z)$ and $w(x,z)$ are determined. The problem is solved for the state $p_z(x) = q_n \sin\xi x$, where $\xi = \frac{n\pi x}{L}$. To this end, the displacements are assumed as:

$$u(x,z) = U(z) \cos \xi x$$
$$w(x,z) = W(z) \sin \xi x \quad (17)$$

Substituting the above displacements in the governing differential Eq. (6) a pair of ordinary differential equations (ODEs) for $U(z)$ and $W(z)$ is obtained for which the following solution forms are considered:

$$U_{(Z)} = \sum_{i=1}^{4} a_i e^{\alpha_i z}, \qquad W_{(Z)} = \sum_{i=1}^{4} b_i e^{\alpha_i z} \quad (18)$$

where α_i is the roots of the characteristic equation of the corresponding ordinary differential equations. The arbitrary constants a_i and b_i are solved using the stress boundary conditions on the top surface of the beam given by Eq. (8) and stress boundary conditions on the bottom of the beam given as the followings:

$$\tau_{zx}(x,0) = 0$$
$$\sigma_{zz}(x,0) = -p_z(x) = -q_n \sin \xi x \quad (19)$$

After calculating the constants a_i and b_i the displacement fields u and w are completely determined. Then, the strains and stresses at any point can be calculated using the strain-displacement and stress-strain relations.

According to the assumed contact stress distribution method [20, 21], the contact is approximated as Hertzian contact (elliptical contact stress distribution) and a one-term function for Eq. (13) is used as [18]:

$$p_z(x) = p_m \sqrt{1 - (\frac{\chi}{b})^2}, \qquad |\chi| < b \quad (20)$$

where p_m is the peak contact stress which is the only unknown. Then, to determine p_m, Eq. (16) takes the following form:

$$p_m(c_0 - c_j) = \frac{\chi_j^2}{2R}, \quad (j = 1, M; \ M \ge N) \quad (21)$$

where c_0 is the displacement w at the center ($x = \frac{L}{2}, z = 0$) and c_j are the displacements w at x_j due to the distribution of the elliptical contact load with $p_m = 1$. The least square error solution of the above equation is obtained as:

$$p_m = \frac{1}{M} \sum_{j=1}^{M} \frac{\chi_j^2}{2R(c_0 - c_j)} \quad (22)$$

p_z can be considered as a Fourier series of the form:

$$p_z(x) = \sum_{n=1}^{\infty} q_n \sin \frac{n\pi}{L} x \quad (23)$$

in which the Fourier coefficients are:

$$q_n = \frac{2}{L} \int_0^L p_z(x) \sin \frac{n\pi x}{L} dx \quad (24)$$

For the Hertzian contact stress in the above equation, the Fourier series coefficients can be as:

$$q_n = \frac{2p_m}{L} \int_0^L \sqrt{1 - \left(\frac{\chi}{b}\right)^2} \sin \frac{n\pi x}{L} dx$$

$$= \frac{2(-1)^{\frac{n-1}{2}} p_m}{L} \int_{-b}^{+b} \sqrt{1 - \left(\frac{\chi}{b}\right)^2} \cos \frac{n\pi \chi}{L} d\chi$$

$$= \frac{2(-1)^{\frac{n-1}{2}} p_m}{n} J_1(\frac{n\pi b}{L}) \quad (25)$$

where J_1 is the first kind Bessel function. In the above calculations, the following equation is used:

$$\int_{-c}^{c} \sqrt{c^2 - x^2} \cos \xi x \, dx = \frac{\pi c}{\xi} J_1(c\xi) \quad (26)$$

3.2. Low Velocity Impact Response

The first step in solving the low velocity impact problem is to achieve the contact force history. As explained in the previous sections, many of the past empirical and analytical studies have shown the relation and similarity between static contact problems and low velocity impact problems. Here, this fact is used to simplify the low velocity impact analysis of the composite beam. The maximum impact force can be related to the initial impact energy as:

$$U = \frac{1}{2} m_i v_i^2 = \frac{1}{2} \frac{F_m^2}{k_b} \tag{27}$$

where m_i and v_i are the mass and velocity of the impactor, respectively, F_m is the maximum impact force and k_b is the bending stiffness of the beam in the case where a concentrated load is applied to its center. In the above energy relation, the strain energy due to the local indentation near the contact is ignored. The bending stiffness of the composite beam is obtained as the following [22]:

$$K_b = \frac{48 D_{11}^*}{L^3} \tag{28}$$

where D_{11}^* is the reduced stiffness.

4. Results

In this section, firstly, the validity of the present analytical modeling is verified. Then, the influences of some key parameters on the indentation and the low velocity impact responses of the composite beam are studied.

The geometrical and mechanical properties of the considered beam are presented in Table 1. Also, unless otherwise stated, it is assumed that the lay-up of the composite beam is [90/90/90/90], the impact velocity is 10 m/s and the impactor diameter is 20 mm.

Table 2 shows the kinetic energy of the impactor at different times. Also, in Table 3, the impact force versus displacement results are presented.

Table 1. Geometrical and mechanical properties of the considered beam

length	L	0.1 *(m)*
ply thickness	h	0.002 *(m)*
modulus of elasticity	E_{xx}	24.51 *(GPa)*
	E_{yy}	7.77 *(GPa)*
	E_{zz}	7.77 *(GPa)*
shear modulus	G_{xy}	3.34 *(GPa)*
	G_{xz}	3.34 *(GPa)*
Poisson's ratio	υ_{xy}	0.078
	υ_{xz}	0.078

As it is seen, there are good agreements between the results obtained from the present research and the results of Ref. [23] which verify the validity and the accuracy of the present analysis.

For lay-up [0/90/0/90] and different values of ply thickness contact force versus indentation curves and distribution of contact pressure curves are illustrated in Figs. 2 and 3 respectively. As it can be observed, increasing the ply thickness, increases the contact force as well as the contact pressure, while it decreases the indentation and also the contact length.

Table 2. Kinetic energy and shear strain values at different times

time (μs)	kinetic energy (J)		
	Ref. [23]	present work	error percentage
0	7.65	7.19	6
50	7.63	7.15	6
100	7.16	6.73	6
150	6.19	5.79	6.5
200	4.91	4.61	6
250	3.37	3.17	6
300	3.26	3.08	5.5

Table 3. Impact force vs. displacement

displacement (mm)	force (kN)		
	present work	Ref. [23]	error percentage
0.1	1.109	1.263	12
0.2	2.033	2.063	1.5
0.3	3.141	3.465	9.5
0.4	3.787	4.181	9.5
0.5	4.842	5.282	8.5
0.6	8.010	8.581	6.5
0.7	7.569	8.533	11
0.8	8.616	10.035	14
0.9	10.435	10.905	4.5
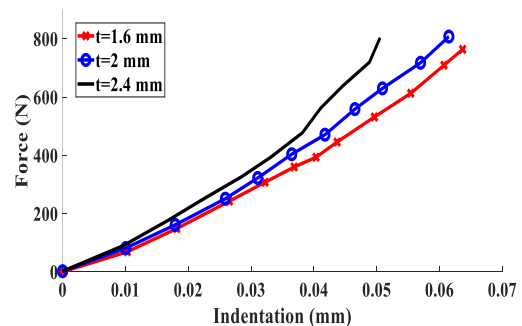
Fig. 2. Contact force versus indentation for different values of ply thickness (lay-up [0/90/0/90])
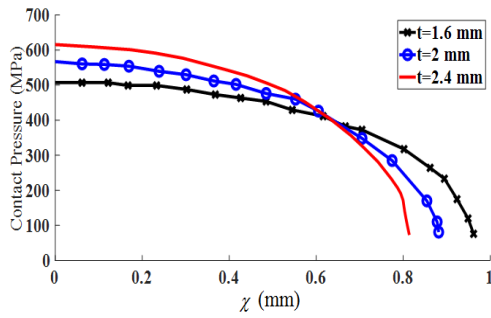
Fig. 3. Distribution of contact pressure for different values of ply thickness (lay-up [0/90/0/90])
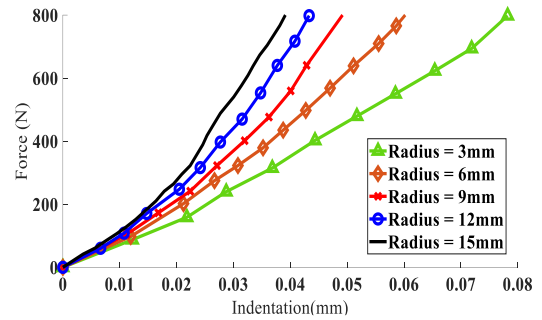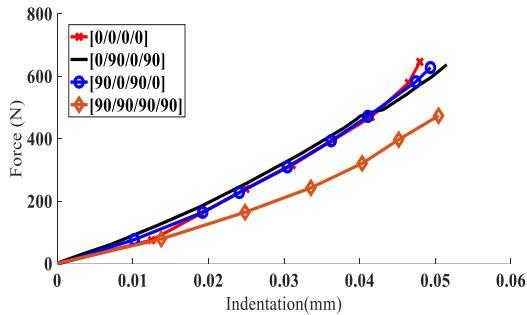
Fig. 4. Contact force versus indentation for different lay-ups
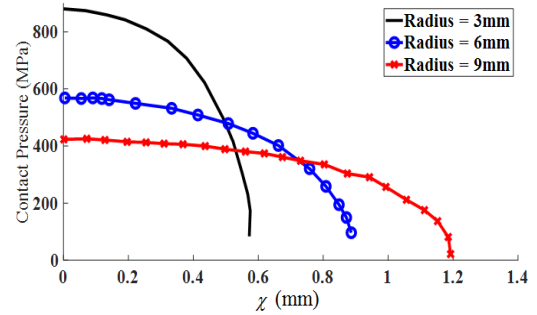
Fig. 5. Distribution of contact pressure at the contact force of 600 N for different lay-ups

Fig. 6. Contact force versus indentation for different values of indenter radius (lay-up [0/90/0/90])
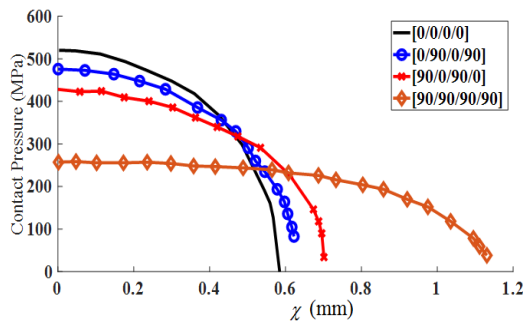
Fig. 7. Distribution of contact pressure for different values of indenter radius (lay-up [0/90/0/90])
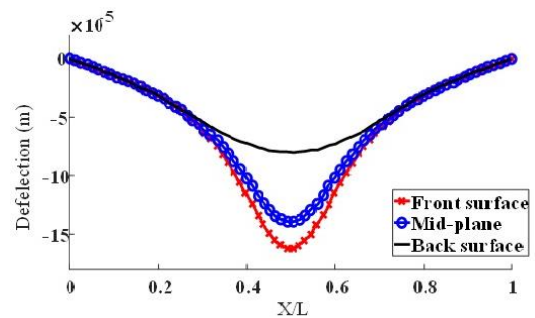
Fig. 8. Deflection of the front surface, the bottom surface, and the midplane of the beam in the longitudinal direction at the maximum impact force (V=1 m/s and L=0.1 m)

Contact force versus indentation curves for different lay-ups are illustrated in Fig. 4. As it can be seen, the curves are very close together except for the case [90/90/90/90] which has less resistance to indentation than the other cases studied. So, choosing a proper lay-up can improve the indentation response of composite beams.

Figure 5 shows the distribution of contact pressure at the contact force of 600 N for different lay-ups. It is observed that the lay-up [90/90/90/90] gives the maximum contact length and the minimum contact pressure, while the lay-up [0/0/0/0] produces the minimum contact length and the maximum contact pressure.

Contact force versus indentation curves for lay-up [0/90/0/90] and different values of indenter radius are shown in Fig. 6. It is seen that as the indenter radius increases, the indentation decreases and the contact force increases.

The distribution of contact pressure for lay-up [0/90/0/90] and different values of indenter radius is presented in Fig. 7. As it is observed, by increasing the indenter radius the contact length increases and the contact pressure decreases.

Deflections of the front surface, the back surface, and the midplane of the beam in the longitudinal direction at the maximum impact force for V=1 m/s and L=0.1 m are shown in Fig. 8. It is seen that the front and the back surfaces find the largest and the smallest deflections, respectively, so that at the center of the beam, the deflection of the front surface is approximately twice the deflection of the back surface.

Maximum indentation versus impact velocity and maximum contact force versus impact velocity curves are illustrated in Figs. 9 and 10 respectively. As it is observed, increasing the impact velocity causes the maximum indentation and the maximum contact force to increase nonlinearly.
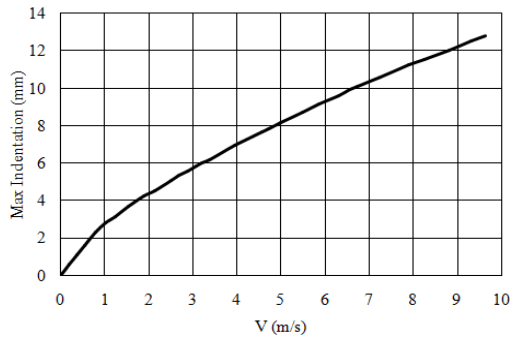
Fig. 9. Maximum indentation versus impact velocity
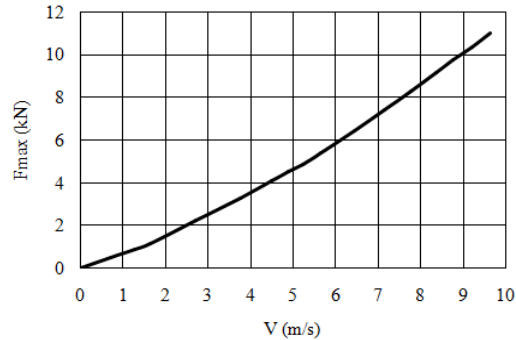
Fig. 10. Maximum contact force versus impact velocity

5. Conclusion

Considering the widespread and increasing use of composite structures and the importance of impact on these structures, in this paper, for the first time, using an assumed contact stress approach, the problem of contact between a rigid cylindrical indenter and a laminated composite beam is analyzed. The analytical results of the relationship between contact force-length and tension were extracted. Then, the results of the beam indentation analysis were generalized to obtain the response of the low velocity impact problem. The results obtained by the presented analytical model were compared and validated with the results that existed in the literature. Also, by performing a parametric study, the influences of important parameters on the indentation and the low velocity impact responses of a composite beam were investigated. The results revealed that with increasing the impact velocity, the maximum indentation and the maximum contact force increase nonlinearly. Also, increasing the ply thickness increases the contact force.

References

[1] Abrate, S., 2005. *Impact on Composite Structure*. Cambridge University Press.

[2] Apetre, N.A., Sankar, B.V. and Ambur, D. R., 2006. Low-velocity impact response of sandwich beams with functionally graded core. International *Journal of Solids and Structures*, *43*, pp. 2479-2496.

[3] Liu, H., Liu, H., and Yang, J., 2017. Clamped sandwich beams with thick weak cores from central impact: A theoretical study. *Composite* Structures, *169*, pp. 21-28.

[4] Ghazifard, P., Najibi, A. and Alizadeh, P., 2019. Numerical Crashworthiness Analysis of Graded Layered Foam-Filled Tubes Under Axial Loading. *Mechanics of Advanced Composite Structures*, *6*, pp. 57-64.

[5] Hertz, H., 1896. On the contact of elastic solids. Paper V of Miscellaneous papers of Hertz collected by Lenard, P., translated by Jones, D.E. and Schott, G.A., MacMillan and Co.

[6] Hertz, H., 1896. On the contact of rigid elastic solids and on hardness. Paper VI of Miscellaneous papers of Hertz collected by Lenard P., translated by Jones, D.E. and Schott, G.A., MacMillan and Co.

[7] Abrate, S., 1991. Impact on Laminated Composite Materials. *Applied Mechanics Reviews*, 44, pp. 155-190.

[8] Abrate,S., 1994. Impact on Laminated Composites: recent advances. *Applied Mechanics Reviews*, *47*, pp. 517-544.

[9] Johnson, W., 1972. *Impact strength of Materials*. Edward Arnold, London.

[10] Mittal, R.K., 1987. A Simplified Analysis of the Effect of Transverse Shear on the Response of Elastic Plates to Impact Loading. *International Journal of Solids and Structures*, *23*, pp. 1191-1203.

[11] Ivañez, I., Barbero, E. and Sanchez-Saez, S., 2014. Analytical study of the low-velocity impact response of composite sandwich beams. *Composite Structures*, *111*, pp. 459-467.

[12] Mines, R., Worral, CM. and Gibson, AG., 1994. Static and Impact Behavior of Polymer Composite Sandwich Beams. *J. Composites*, *25(2)*, pp. 95-110.

[13] Tan, TM. and Sun, CT., 1985. Use of statical indentation laws in the impact analysis of laminated composite plates. *J Appl Mech*, *52(1)*, pp. 6–12.

[14] Sankar, BV. and Sun, CT., 1985. An efficient numerical algorithm for transverse impact problems. *Comput Struct*, *20(6)*, pp. 1009–12.

[15] Kwon, YS., and Sankar, BV., 1993. Indentation-flexure and low-velocity impact damage in graphite/epoxy laminates. *ASTM J Compos Technol Res*, *15(2)*, pp. 101–11.

[16] Sankar, BV. and Sun, CT., 1985. Low-velocity impact response of laminated beams subjected to initial stresses. *AIAA J*, *23(12)*, pp. 1962–9.

[17] Sankar, BV., 1992. Scaling of low-velocity impact for symmetric laminates. *J Reinf Plast Compos*, *11(3)*, pp. 296–309.

[18] Yalamanchili, V.K. and Sankar, B.V., 2012. Indentation of functionally graded beams and its application to low-velocity impact response. *Composites Science and Technology*, *72*, pp. 1989–1994.

[19] Autar, K. K., 2006. *Composite Materials*. Taylor and Francis Group, CRC Press.

[20] Sankar, BV., 1989. Smooth indentation of orthotropic beams. *Compos Sci Technol*, *34(2)*, pp. 95–111.

[21] Sankar, BV., 1989. An integral equation for the problem of smooth indentation of orthotropic beams. *Int J Solids Struct*, *25(3)*, pp. 327–37.

[22] Sankar, BV., 2001. An elasticity solution for functionally graded beams. *Compos Sci Technol, 61*, pp. 689–696.

[23] Tanay Topac, O., Gozluklu, B., Gurses, E. and Coker, D., 2017. Experimental and computational study of the damage process in CFRP composite beams under low-velocity impact. *Composites Part A: Applied Science and Manufacturing*, *92*, pp. 167–182.